J Mater Sci (2010) 45:5642–5648
DOI 10.1007/s10853-010-4629-7

Evaluation of oxidation resistance of thin continuous silicon oxycarbide fiber derived from silicone resin with low carbon content

Masaki Narisawa · Ryu'ichi Sumimoto · Ken'ichiro Kita

Received: 30 March 2010 / Accepted: 17 May 2010 / Published online: 4 June 2010

Abstract Si–O–C ceramic fiber was synthesized from a kind of silicone resin with low carbon content. The melt-spun resin fiber was exposed to $SiCl_4$ vapor under a nitrogen gas flow, and the fiber was heated at 373 K for 2 h to complete the curing process. The cured fiber was pyrolyzed at 1273 K in an inert atmosphere to be converted to Si–O–C fiber. The entire chemical composition of the pyrolyzed fiber was almost identical to that of a previously reported resin which was pyrolyzed without curing. Auger spectrum analysis indicated an increase in silicon content near the fiber surface. The Si–O–C fiber thus obtained was heat-treated at 1511 or 1603 K in an air flow to evaluate oxidation resistance. Elemental analysis, XRD measurement, and SEM image observations were carried out on the oxidized Si–O–C fibers. Even with such thin fiber diameters, the oxidation process under these conditions was slow and the formation of a thin oxide layer on the fiber surface was confirmed. The existence of a residual Si–O–C core surrounded by a crystallized silica layer was observed in fractured fiber cross-sections after severe treatment conditions of 24 h oxidation at 1511 K or 3 h oxidation at 1603 K.

Introduction

Silicon oxycarbide (Si–O–C) materials have recently attracted wide interest [1–5]. It has been reported that Si–O–C materials show high creep resistance two orders of magnitude higher than that of silica in the temperature range of 1273–1473 K [6]. In addition, it has long been known that a protective silica layer is formed on the surface of Si–O–C materials during oxidation [7]. Brewer et al. analyzed the efficiency of the silica layer in terms of free carbon content and number of remaining Si–C bonds in the pyrolyzed Si–O–C powder samples. Low carbon content and increase in Si–C bonds improved the efficiency of the silica layer in protecting the materials [8].

On the other hand, it is known that densely cross-linked silicone resins with methyl groups are synthesized mainly from CH_3SiCl_3, which is produced on a large scale as a by-product in the silicone industry [9]. The polymerization of CH_3SiCl_3 does not require any kinds of special reagent, such as sodium or magnesium [10, 11]. This suggests that polymethylsilsesquioxane (PMSQ)-like resins derived from CH_3SiCl_3 could become widely commercialized, like linear silicones presently used as the heat-resistant oils, resins, and elastomers, owing to their intrinsically low cost. For example, various kinds of resins named PMSQ are currently commercialized in the field of cosmetics.

We recently succeeded in synthesizing thin continuous Si–O–C fibers from a melt spinnable PMSQ-like resin [12, 13]. In this method, the spun fiber was cured by $SiCl_4$ vapor, which reacted with the residual silanol groups in the resin. In 1987, another kind of Si–O–C fiber was synthesized from a silsesquioxane copolymer with phenyl and vinyl side groups [14]. However, the ultraviolet (UV) curing process adopted in this case intrinsically required phenyl groups in the chain structure with absorption bands in the UV range [15]. Therefore, the expected carbon content in the Si–O–C fiber obtained by UV curing was thought to be high. The $SiCl_4$ curing process adopted in our procedure does not require phenyl groups, and hence the carbon content in the obtained fiber is reduced.

M. Narisawa (✉) · R. Sumimoto · K. Kita
Graduate School of Engineering, Osaka Prefecture University, Sakai, Osaka 599-8531, Japan
e-mail: nar@mtr.osakafu-u.ac.jp

A few previous studies have been conducted on Si–O–C fibers with low carbon content, synthesized by the sol–gel method [16, 17]. Compared to dry-spun procedure via the sol–gel method, our method which is based on a silicone resin melt-spinning process has an advantage in wide industrial application. In this article, the oxidation resistance of Si–O–C fibers derived from a silicone resin with low carbon content is described within the contexts of residual carbon content, protective silica layer formation on the surface, and slow crystallization process.

Experimental procedure

Si–O–C fiber synthesis

Commercialized silicone resin (YR3370, Momentive Performance Materials Japan) was prepared for the melt-spinning process. The analyzed chemical composition of the resin was $SiO_{1.78}C_{1.22}H_{3.67}$. The silicon and carbon contents were analyzed on the basis of JIS R 1616, while the hydrogen content was analyzed by the inert gas fusion method. The ^{29}Si NMR spectrum indicated the major signal at −65 ppm assigned to $SiCO_3$ (T) and a shoulder at −57 ppm assigned to $CSi(OSi)_2(OH)$ (T_2). The IR spectrum indicated absorption bands at 3400, 1250, 1100, 1020, and 820 cm^{-1}, assigned to the O–H, Si–CH_3, Si–O–Si, Si–O–Si, and Si–C bonds, respectively [16]. These results suggested that –$Si(CH_3)O_{1.5}$– was the main unit and that additional OH groups were present in the resin's molecular structure. The carbon content was, however, somewhat higher than expected. In addition to OH groups, the existence of methoxyl terminal groups may explain the high carbon content. However, this cannot be ascertained from the observed spectra.

The resin was melt-spun to fiber form at 423 K under the conditions described in a previous article [12]. A bundle of 200 mg of the spun fiber 100 mm in length was placed in a glass tube in a diameter of 70 mm, and the tube was purged by nitrogen gas to avoid effects of moisture. In a deep glass dish, 10 mL of $SiCl_4$ liquid was prepared in a purged glove bag and placed in the same tube 350 mm away from the fiber zone. After controlling the flow rate of the purge gas from the $SiCl_4$ zone to the fiber zone at 50 mL/min, the fiber zone was heated to 373 K at a rate of 40 K/h and held at this temperature for 2 h.

The cured fiber was pyrolyzed in an Ar gas flow of 300 mL/min at a heating rate of 300 K//h and a holding time of 1 h at 1273 K. Elemental analysis was performed on a fiber with a whole mass of 100 mg. The Si content was analyzed with an ICP-AES (SPS4000, Seiko Instruments Inc.). The oxygen content was analyzed by an inert gas fusion–IR absorption instrument (LECO TC-136, LECO Corporation). The carbon content was analyzed by a high frequency combustion–IR absorption instrument (LECO IR-412, LECO Corporation). Each analysis was carried out two or three times. The margin of error for the estimated values was less than 1 mass%. Elemental analysis of the fiber surface was performed by Auger electron spectroscopy (PHI 670Xi, Physical Electronics, Inc.) with etching via Ar ion bombardment. The estimated etching rate was 6.0 nm/min based on the silica standard. The tensile strength of the fiber was measured using a tensile testing machine (Tensilon UTM-II, Toyo Measuring Instruments) equipped with a 0.1 kgf load cell (TLU-0.1L-F2, ORIENTEC) with a gauge length of 10 mm and a crosshead speed of 2 mm/min. The resulting tensile strength was expressed as an average of 20 individual monofilaments.

Oxidation resistant tests on the Si–O–C fiber

The pyrolyzed Si–O–C fiber was placed in an electric furnace equipped in $MoSi_2$ heaters. Air was introduced in an alumina tube with a diameter of 45 mm at a flow rate of 300 mL/min. The fiber was heated at 1511 and 1606 K. The heating rate was 300 K/h, and the holding times were 1 min, 3 h, and 24 h for 1511 K, and 3 h for 1606 K. Silica fiber (Quartz fiber, SOGO LABORATORY GLASS WORKS CO., LTD., expected purity >99.9%) was prepared as a reference and heat-treated under the same conditions.

The fibers obtained after these heat treatments were analyzed by XRD (RINT-1100, Rigaku). The fracture surface and fiber bundle surface were observed using a FE-SEM (S-4500, Hitachi) or a FE-SEM (S-4800, Hitachi) equipped with EDX (Genesis XM 2, AMETEK Inc.).

Result and discussion

Characterization of synthesized Si–O–C fibers

The mass gain of the spun fiber after 2-zone $SiCl_4$ curing process was 5.5 mass%, which was larger than that of the previous 1-zone curing process at 313 K (2.0 mass%). It indicates that the resin fiber captured much of the $SiCl_4$ during the curing process at 373 K. The ceramic yield of the cured fiber after pyrolysis at 1273 K was 89%. The analyzed chemical composition of the fiber was $SiO_{1.49}C_{0.65}$, while the reported chemical composition of pyrolyzed bulk resin sample at 1473 K was $SiO_{1.5}C_{0.68}$ [18]. The entire chemical composition of the fiber was roughly the same as that of the pyrolyzed resin. The diameter of the obtained Si–O–C fiber was 13.4 ± 1.8 μm, and the tensile strength was 0.56 ± 0.29 GPa; latter was a little higher than that of a previous Si–O–C fiber obtained by the 1-zone curing

process (0.30 ± 0.13 GPa). Every fiber was colored black and appeared thin and straight. One reason for the observed low strength may be heterogeneity in the curing process, since fibers with higher tensile strength (0.7 GPa) were obtained by radiation curing of melt-spun resin fibers [13]. Even for metal chloride curing, further increase in tensile strength will be possible by adjusting curing conditions. In spite of the low carbon content in the resin precursor, however, the pyrolyzed Si–O–C fiber contains a considerable amount of excess carbon in the structure. This excess carbon possibly acts as defects in the fiber. In order to achieve tensile strengths in the range of 2–3 GPa (like those for conventional glass fibers), reducing the excess carbon will be necessary.

Auger spectrum analysis of the Si–O–C fiber surface is shown in Fig. 1. Up to a depth of 20 nm, the oxygen content is apparently high. This is possibly results of contamination on the fiber surface. In addition to contamination, the silicon content is rather high and the carbon content is low near the fiber surface. The averaged elemental composition at a depth of 40–140 nm was $SiO_{0.94}C_{0.33}$, while that at a depth of 500–600 nm is $SiO_{1.02}C_{0.57}$. These values are inconsistent with the chemical composition of the whole fiber. An effect of $SiCl_4$ capture on the increase in Si content is likely near the fiber surface.

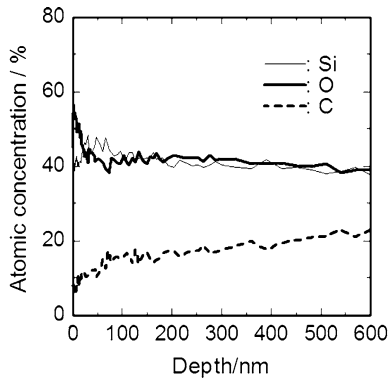

Fig. 1 Auger analysis of the Si–O–C fiber surface (Etching rate of 6.0 nm/min with using silica standard)

Results of the oxidation resistance tests

Figure 2a and b shows the XRD patterns for the Si–O–C and reference silica fibers after heat treatment in an air flow. The XRD pattern for the Si–O–C fiber before oxidation is similar to that for the amorphous silica fiber. The peak is, however, broadened to around 22°. The broadness is apparent when compared to that of the silica fiber.

Although crystallization of amorphous silica fiber to form cristobalite proceeds even after a holding time of 1 min, signals of cristobalite in the Si–O–C fiber are very weak after 1 min holding. This indicates that oxidation of the Si–O–C fiber is insubstantial during the heating up to 1511 K. Even after 3 h, the major broad line is maintained apart from the growth of cristobalite. After 24 h, the XRD pattern of the Si–O–C fiber becomes almost identical to that of the silica fiber. The fiber bundle, however, maintains a black color.

Figure 3a–c shows SEM images of the Si–O–C fiber after heat treatment at 1511 K. After a holding time of 1 min, there is almost no change in the appearance of the fiber. After 3 h, fusing of the Si–O–C monofilaments is frequently observed, although the surface retains smooth appearance. After 24 h, tiny cracks are formed on the fused fiber bundles. The fibers, however, usually keep a straight shape even with a fusing of the surface. On the other hand, the silica fiber is broken into short cylinders even after 1 min of heat treatment (Fig. 3d). The silica fiber is thought to be degraded severely during the increase in temperature to 1511 K. After a holding time of 3 h, the

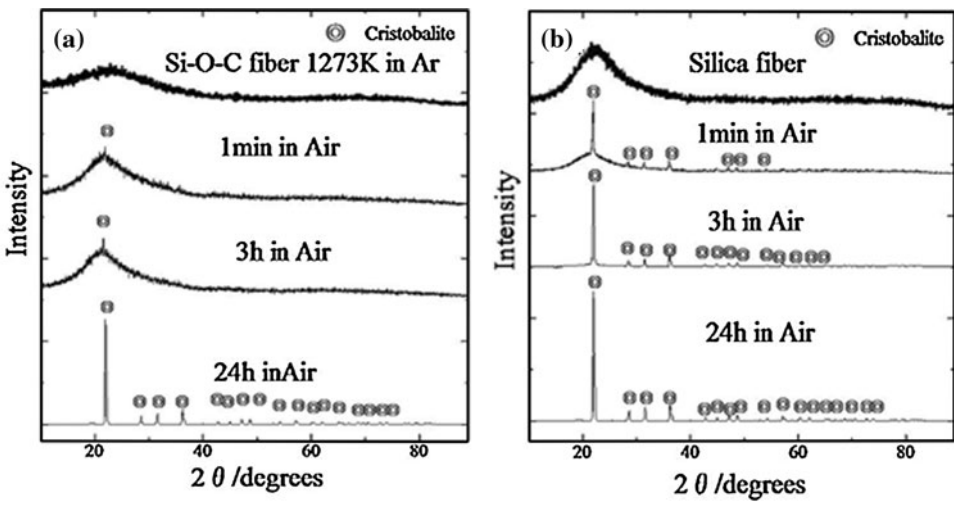

Fig. 2 XRD patterns of inorganic fibers after heat treatment at 1511 K in an air flow; **a** Si–O–C fiber, **b** silica fiber

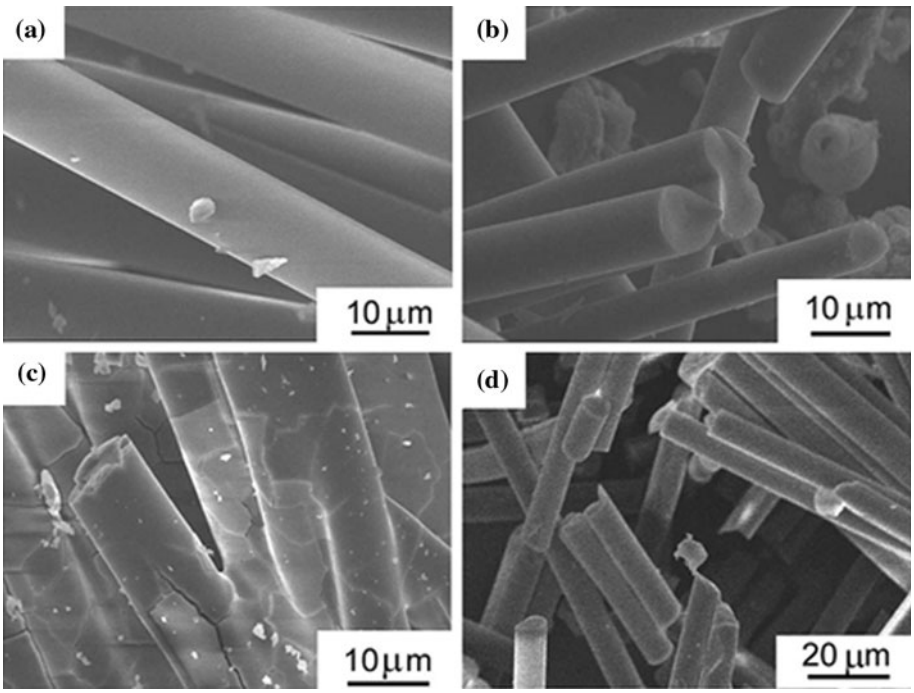

Fig. 3 SEM images of inorganic fiber after heat treatment at 1511 K; **a** Si–O–C 1 min, **b** Si–O–C 3 h, **c** Si–O–C 24 h, **d** silica 1 min

silica fiber bundle is completely fused. It is difficult to find monofilament shapes in the heat-treated sample.

In Table 1, the results of the elemental analysis of the Si–O–C fiber after 3 h of oxidation at 1511 K are shown along with reference data of the original Si–O–C fiber and the starting resin. The residual carbon content is 62% of the original value. When considering the small diameter of the synthesized fiber, this value is extremely high. In addition to the decrease in carbon content, the oxygen content in the fiber increases from 1.5 to 1.7. The latter may corresponds to the surface silica formation. When a homogeneous Si–O–C rod with a diameter of 13.6 μm and infinite length is assumed as a model of the starting Si–O–C fiber, a 38% decrease in carbon content corresponds approximately to silica layer with a thickness of 1.5 μm from the fiber surface. In this approximation, the density of Si–O–C is assumed to be same as that of the amorphous silica.

Figure 4 shows cross-section of Si–O–C fibers after heat treatment up to 1511 K. After 3 h, the formation of a silica layer is not observable despite the considerable oxidation of the fiber. Since Si–O–C and silica are insulators, it is difficult to observe the interface of these materials from ordinary SEM images. On the other hand, fibers heat-treated for 24 h show the formation of a silica layer with a thickness of 4 μm. The clear interface around the Si–O–C core suggests de-bonding between the core and the layer. Such de-bonding is probably caused by the growth of the cristobalite and changes in the volume of the formed layer.

Figure 5a and b shows the XRD pattern and SEM image, respectively, of the Si–O–C fiber heat-treated for 3 h at 1606 K. The growth of cristobalite is observed on the broad Si–O–C pattern (Fig. 5a). From the perspective of silica layer crystallization, this state is located between 3 and 24 h treatment at 1511 K. Most of the cross-sections of the monofilaments are smooth, and it is difficult to observe the silica layer. In a few cases, the silica layer becomes observable in cross-sections as shown in Fig. 5b. Under these conditions, de-bonding between the Si–O–C core and the surrounding silica layer is rare despite considerable cristobalite growth.

Figure 6a and b shows a line analysis by EDX on a cross-section of the S–O–C fiber after 3 h oxidation at 1606 K. A smooth cross-section without any remarkable structures was selected for the analysis. The line analysis on the cross-section reveals an increase in oxygen content within a few micrometers of the fiber surface. These results

Table 1 Results of elemental analysis of the resin, Si–O–C fiber and oxidized Si–O–C fiber (1511 K for 3 h in air)

Sample	Si (mass%)	O (mass%)	C (mass%)	H (mass%)	Composition
Silicone resin	37.5	38	19.6	4.9	$SiO_{1.78}C_{1.22}H_{3.67}$
Si–O–C fiber	47	40	13	–	$SiO_{1.49}C_{0.65}$
Oxidized fiber	46	46	8	–	$SiO_{1.76}C_{0.41}$

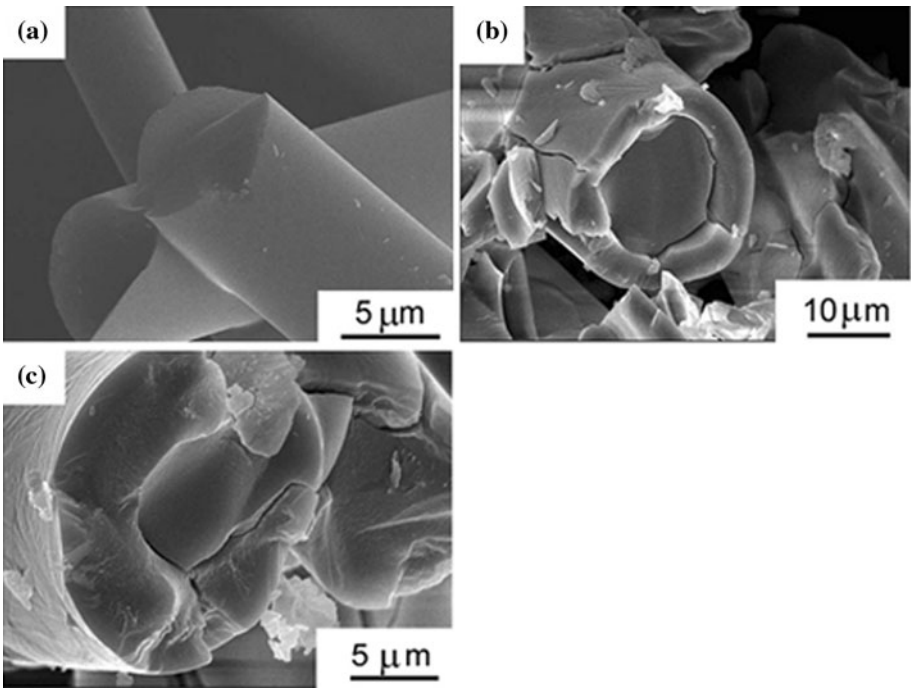

Fig. 4 SEM images of cross-sections of the Si–O–C fibers after 1511 K heat treatment; **a** 3 h, **b** 24 h-1, **c** 24 h-2

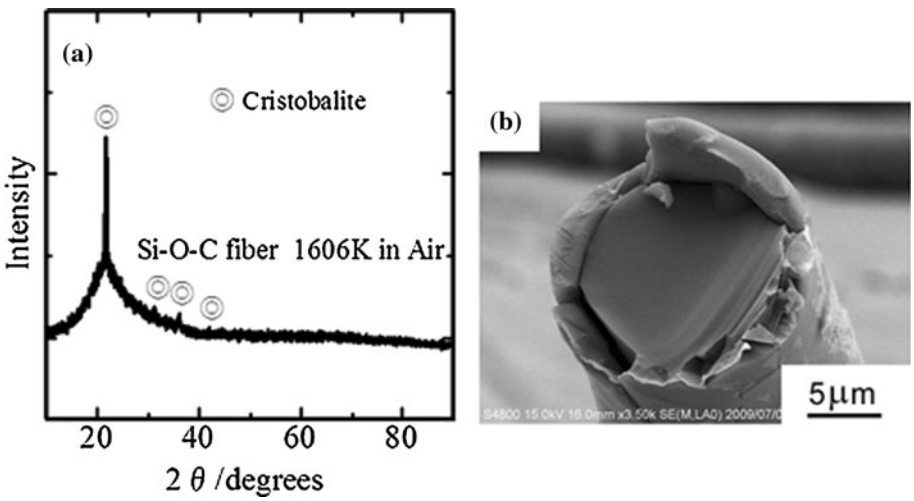

Fig. 5 **a** XRD pattern and **b** cross-sections of the Si–O–C fiber after heat treatment at 1606 K for 3 h

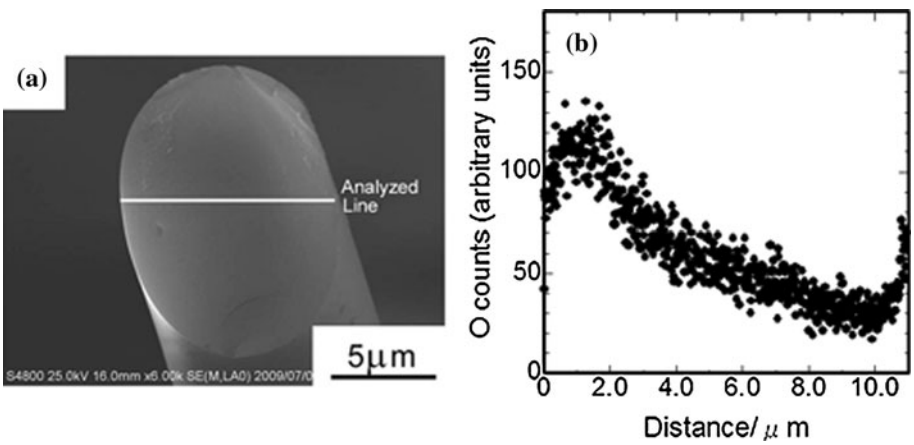

Fig. 6 **a** Smooth cross-section of the Si–O–C fiber after heat treatment at 1606 K for 3 h in air, and **b** line analysis of O (Kα) along the fiber cross-section

suggest that despite the lack of any structural differences, a silica layer exists on the fiber surface.

It is known that such silica layers often protect Si base materials from rapid oxidation [19, 20]. In the presence of the layer, the oxygen diffusion process within the layer typically comes to control the rate of oxidation, and the oxidation kinetics is then expressed by a parabolic law [21]. It is undoubtedly the major factor in delayed oxidation of Si–O–C fibers synthesized from silicone resin.

The efficiency of the silica layer on Si–O–C fibers is inferior to that on commercialized Si–C fibers [22, 23]. Figure 7 shows the cross-section of a Si–C fiber (Hi-Nicalon, Nippon Carbon ($SiC_{1.39}O_{0.01}$)) after 60 h of air oxidation at 1573 K. Even under such a severe environment, the estimated thickness of the silica layer is ca. 0.3–0.4 μm. It is suggested that the silica layer formed on the Si–O–C fiber is not dense and is thickened more easily than on the Si–C fiber.

In comparing the Si–O–C fiber and Si–C fibers, a major factor determining the efficiency of the silica layer may be the state of carbon within the fibers.

$$SiO_{1.49}C_{0.65} \rightarrow 0.75SiO_2 + 0.25SiC + 0.40C \quad (1)$$

$$SiC_{1.39}O_{0.01} \rightarrow SiC + (SiO_2)_{trace} + 0.39C \quad (2)$$

Equations 1 and 2 express the chemical compositions of thermodynamically stable phases derived from amorphous fibers. In terms of chemical composition, the free carbon content in the Si–O–C fiber is not substantially different from that in the Si–C fiber. However, the segregation of turbostratic carbon from the Si–C amorphous network in the Si–C fiber requires heat treatment at 1673 K [24]. On the other hand, the compatibility of excess carbon and silica networks in amorphous Si–O–C is expected to be low. Raj et al. proposed a structural model of an excess carbon network, which surrounds the Si atom coordination center in amorphous Si–O–C [25]. In the case of Si–O–C, the process of silica layer formation is continuously exposed to the evolution of CO gas. Perhaps, continuous CO evolution prevents densification of the silica layer. Such an understanding of the oxidation process is consistent with previous results observed by Brewer et al. [8].

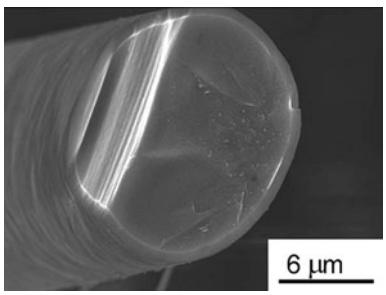

Fig. 7 Fractured cross-section of Hi-Nicalon fiber heat-treated for 60 h at 1573 K in air

Based on these comparisons, the Si–O–C fiber synthesized here is positioned as "lower grade ceramic fiber" relative to commercialized Si–C fibers in terms of appearance. Although the mechanism of heat resistance is similar to that of ordinary Si–C fibers, the absolute efficiency of the protective silica layer is inferior. Nonetheless, the oxidation resistance at high temperatures is quite practical and meaningful for industrial uses. The intrinsically low cost of the original resin makes it attractive as a potentially "conventional" material. Application to filters, heat insulators and heat radiators at reduced costs is promising in temperature range of 873–1473 K. Since thickening of the silica layer is unremarkable even at 1606 K for up to 3 h, disposable high-temperature materials with a short life-time could be a unique application. In addition, the process of Si–O–C fiber synthesis intrinsically accepts various doping elements through vapor during the processes of curing and pyrolysis. Since the idea is simple and the procedure is easy, there is little doubt that there will be further development in the fiber synthesis process toward tailored chemical composition, improved heat resistance and increased tensile strength.

Conclusion

By using the 2-zone curing method and exposing silicone resin fiber to $SiCl_4$ vapor under controlled pressure, a resin fiber with an increased amount of the captured $SiCl_4$ is obtained. After pyrolysis, Si–O–C fiber with a chemical composition of $SiO_{1.49}C_{0.65}$ and a tensile strength of 0.56 ± 0.29 GPa are obtained.

During heating at 1511 or 1606 K in an air flow, the Si–O–C fiber is not simultaneously oxidized. Oxidation, apparent creep, and growth of cristobalite in the Si–O–C fiber are extremely slow despite small diameter of the fibers. Even after 24 h of oxidation at 1511 K, Si–O–C cores with a diameter of 5 μm surrounded by a 4 μm silica layer are observed. After 3 h of heat treatment at 1606 K, the confirmed silica layer thickness is 2 μm. Since the electrical nature of Si–O–C is similar to silica, this silica layer is not easily observable, unless it is highly crystallized. Although considerable CO evolution from the fiber core prevents the densification of the silica layer, the existence of a surface silica layer protects the Si–O–C core from rapid oxidation.

Acknowledgements This work is partly supported by a Grant-in Aid for Scientific Research C (No. 20560627) from Japan Society of Promotion Science. We thank to Professor Young-Wook Kim (The University of Seoul) for information about physical–mechanical properties of YR 3370 resin.

References

1. Burns GT, Taylor RB, Xu Y, Zangvil A, Zank GA (1992) Chem Mater 4:1313
2. Hurwitz FI, Heimann P, Farmer SC, Hembree DM Jr (1993) J Mater Sci 28:6622. doi:10.1007/BF00356406
3. Soraru GD, D'Andrea G, Campostrini R, Babonneau F, Mariotto G (1995) J Am Ceram Soc 78:379
4. Wilson AM, Zank G, Eguchi K, Xing W, Yates B, Dahn JR (1997) Chem Mater 9:2139
5. Colombo P, Modesti M (1999) J Am Ceram Soc 82:573
6. Rouxel T, Soraru GD, Vicens J (2001) J Am Ceram Soc 84:1052
7. Renlund GM, Prochazka S, Doremus RH (1991) J Mater Res 6:2716
8. Brewer CM, Bujalski DR, Parent VE, Su K, Zank GA (1999) J Sol-Gel Sci Technol 14:49
9. Rochow EG (1987) Silicon and silicones. Springer-Verlag, Heidelberg, Germany
10. Suminoe T, Matsumura Y, Tomomitsu N (1978) Japan Patent S53-88099
11. Baney RH, Itoh M, Sakakibara A, Suzuki T (1995) Chem Rev 95:1409
12. Narisawa M, Sumimoto R, Kita K, Kado H, Mabuchi H, Kim YW (2009) J Appl Polym Sci 114:2600
13. Narisawa M, Sumimoto R, Kita K, Mabuchi H, Kim YW, Sugimoto M, Yoshikawa M (2009) Adv Mater Res 66:1
14. Hurwitz FI, Hyatt L, Gorecki J, D'Amore L (1987) Ceram Eng Sci Proc 8:732
15. West R, Lawrence DL, Djurovich PI, Yu H, Sinclair R (1983) Ceram Bull 62:899
16. Kamiya K, Katayama A, Suzuki H, Nishida K, Hashimoto T, Matsuoka J, Nasu H (1999) J Sol-Gel Sci Technol 14:95
17. Sorarù GD, Dirè S, Berlinghieri A (May 6, 2004) US Patent 2004/0087431 A1
18. Narisawa M, Yasuda H, Mori R, Mabuchi H, Oka K, Kim YW (2008) J Ceram Soc Japan 116:121
19. Opila EJ (1999) J Am Ceram Soc 82:625
20. More KL, Tortorelli PF, Ferber MK, Keiser JR (2000) J Am Ceram Soc 83:211
21. Hulbert SF (1969) J Brit Ceram Soc 6:11
22. Shimoo T, Chen H, Okamura K (1992) J Ceram Soc Japan 100:929
23. Kakimoto K, Shimoo T, Okamura K (1998) J Am Ceram Soc 81:409
24. Bouillon E, Mocaer D, Villeneuve JF, Pailler R, Naslain R, Monthioux M, Oberlin A, Guimon C, Pfister G (1991) J Mater Sci 26:1517. doi:10.1007/BF00544661
25. Saha A, Raj R, Williamson DL (2006) J Am Ceram Soc 89:2188